PHYSICAL REVIEW A VOLUME 27, NUMBER 6 JUNE 1983

Broadening of Lyman lines of hydrogen and hydrogenic ions by low-frequency fields in dense plasmas

Robert Cauble
Berkeley Research Associates, Springfield, Virginia 22151

Hans R. Griem
Laboratory for Plasma and Fusion Energy Studies, University of Maryland, College Park, Maryland 20742
(Received 22 November 1982)

A previously developed extension of the quasistatic approximation which allows for the broadening of hydrogen lines by low-frequency fields is applied to the first four Lyman lines of hydrogen, ionized helium, C VI, and Ar XVIII. It is demonstrated numerically that the low-frequency Stark broadening is Gaussian in the case of relatively small dynamical corrections. Extrapolation of this Gaussian approximation to cases with large corrections leads to good agreement with measurements of the Lyman-α, -β, and -γ lines of hydrogen and allows the prediction that the Lyman-δ should retain its central dip.

I. INTRODUCTION

Profiles of spectral lines, broadened mostly by Stark effects from electric fields produced by charged particles in dense plasmas, have long been used for determining electron or ion densities and related quantities (like the surface gravities of stars). A much more recent application is the measurement of deuterium-tritrium (DT) fuel densities in inertial fusion experiments from profiles of x-ray lines emitted by small admixtures of suitable heavier elements, e.g., argon. Because lines of one-electron systems, being subject to linear Stark effects, are especially sensitive to the perturbations caused by charged particles, hydrogen lines are most useful in the analysis of stellar atmospheres and Ne X or Ar XVIII lines in the inertial-confinement fusion experiments. Almost as suitable are He I and lines from heliumlike (two-electron) ions having upper levels with close perturbing levels within about a line width.

Experimental verifications[1] of line broadening calculations[2,3] for hydrogen lines generally indicated $\sim 10\%$ accuracy in electron density determinations from Balmer lines. However, experiments also revealed some discrepancies in the central profile regions of such lines[4] and much larger discrepancies for Lyman lines.[5] If, e.g., Lyman-α had been used for density diagnostics, an error of over a factor of 2 would have been incurred in the sense of an overestimate.

Since the discrepancies depended on the (reduced) perturber mass,[4] it was natural to seek as their cause deviations from the quasistatic approximation for the broadening by ions. Various attempts were made to allow for the dynamics of ion-radiator interactions, most of them being reviewed in Ref. 6. Of these attempts, an analytic approximation procedure developed by one of us[7] allows systematically for the first time derivatives of the perturbing fields produced by ions and by low-frequency collective modes. The required joint probabilities for the squares of these derivatives and the initial field acting on the radiator were obtained by combining Chandrasekhar and von Neumann's fluctuation moments[8] for gravitational fields produced by stochastically distributed and independently moving stars with a fluid model for the collective fluctuations. [See Appendix of Ref. 7, but note that in the last equation the exponent of the first $k\rho_D$ factor should be 4 and that the factor in square brackets should be -2. Also, as already pointed out in Ref. 9, the coefficient of the $\tan^{-1}(x_m/\sqrt{2})$ term in the collective contribution should be multiplied by 3 to obtain the correct expression as used in the previous and present calculations.]

It is hoped that our statistical model will soon be subjected to experimental tests via light scattering or computational tests via two-component plasma simulations. Pending such tests, we can point out the excellent agreement obtained both for Lyman-α[7] and Lyman-β,[9] notwithstanding the very different profile structures and the required extrapolation of the small-time expansion for the low-frequency field effects in case of Lyman-α. This extrapolation will be discussed in more detail in Sec. II, together with other aspects of the calculations.

Our new results given in Sec. III show that the excellent agreement with experiment[10] is also obtained for Lyman-γ, and we can now predict that dynamical effects should not be sufficient to smear out the central dip of Lyman-δ under the conditions of the various experiments.[4,5,10]

Encouraged by the good correspondence between measured and calculated profiles of hydrogen lines, we present in Sec. III calculated profiles and profile parameters for one-electron ion lines as well. Although almost no experimental verification is available for these lines, it seems nevertheless reasonable to expect similar accuracy as for hydrogen lines, because the relevant dimensionless parameters have very similar values.

II. THEORY AND CALCULATIONS

To obtain the line shape, the time-dependent Schrödinger equation (already averaged over the fast electron time scale) must be solved for the radiator in some initial field which then varies with time. For Lyman-α, this was done[7] for the unshifted components, assuming the shifted components to be much broader than the electron collision width of the unshifted components. For Lyman-β, the coupled upper-state equations were solved[9,11] by Fourier transforming and algebraically iterating to second order in the field derivatives. Application of the latter method in the present paper to the Lyman-α, -γ, and -δ lines is straightforward, but in the cases of $n=4$ and $n=5$ quite tedious. Use was made of the symbolic manipulation program MACSYMA (Mathlab Group, Massachusetts Institute of Technology, Cambridge, MA) to facilitate the algebra, the details of which can be found in the Appendix. The average over initial fields and field derivatives was done numerically.

If the detuning $\Delta\omega$ is measured in terms of the shift of the innermost shifted Stark component in the Holtsmark field F_0, i.e., in terms of

$$\omega_n=\frac{3n\hbar}{2Zme}F_0\approx\frac{3n\hbar}{2Zmr_0^2}=\frac{3n\hbar}{2Zm}\left[\frac{4\pi N}{3}\right]^{2/3},$$

where n is the upper-state principal quantum number, the profile correction can be written as

$$\Delta l(x_n)=\omega_n\Delta L(\omega)=\epsilon_n^{(1)}E_c^{(1)}(x_n)+\epsilon_n^{(2)}E_c^{(2)}(x_n)\ . \tag{1}$$

Here $x_n=\Delta\omega/\omega_n$, and $\Delta l(x_n)$ is the field averaged, but not radiator velocity averaged profile correction; $E_c^{(1,2)}(x_n)$ are functions of the electron collision width C. The quantities $\epsilon_n^{(1,2)}$ are given by

$$\epsilon_n^{(1)}=\left[\frac{2mZr_0v}{3n\hbar}\right]^2 \tag{2a}$$

and

$$\epsilon_n^{(2)}=\left[\frac{2mZr_0}{3n\hbar}\right]^2\frac{3k_BT}{M_i}\ , \tag{2b}$$

where v is the radiator velocity, which must be included in the average over velocities, and M_i is the mass of the perturbing ions. The line-shape correction can be seen to consist of two terms, the first of which dominates in the case of light emitters perturbed by much heavier ions (for example, hydrogen broadened by argon). The first term in Eq. (1) is negligible in the case where light ions cause broadening in a heavy emitter (e.g., argon in a DT plasma).

Since the interaction term in the Schrödinger equation is approximated by a function linear in time t the derived second-order expression in Eq. (1) is correct only to second order in t. This may not be adequate in the case where the decay times from electron collisions are long, i.e., when C is small. If C/ω_n is a small number, the implicit assumption of nonoverlapping electron and ion time scales may not be valid. To model terms in the correction of order greater than t^2, we will make the extrapolation in Eq. (3).

Greene[12] has shown that the small-time dependence of the conditional covariance, which governs the part of the line shape due to ion broadening, is quadratic in time. We conjecture that this is the small-time limit of a Gaussian, i.e.,

$$L_G(t)\approx e^{-Ct}e^{-\omega_G^2/4t^2}\rightarrow e^{-Ct}(1-\tfrac{1}{4}\omega_G^2t^2)\ , \tag{3}$$

where the time domain line shape is given in terms of an effective electron collision width C and a Gaussian profile of $1/e$ width ω_G. The Fourier transform of the short-time (second-order) correction in Eq. (3) is

$$\Delta L_G(\omega)\simeq\frac{1}{\pi}\frac{\omega_G^2}{4}\frac{C^3-3C(\Delta\omega)^2}{[C^2+(\Delta\omega)^2]^3}\ . \tag{4}$$

Our second-order solution of Eq. (1) turns out to have the same form as Eq. (4) for the four Lyman lines studied so far, except for an overall change of sign for $n=3$ and 5. Letting $\omega_G^2\equiv 4b(\epsilon^{(1)}+\epsilon^{(2)})\omega_n^2$ and noting that at $\Delta\omega=0$, $E_c^{(1)}(\Delta\omega)=E_c^{(2)}(\Delta\omega)$, we find that

$$b=\pi\,|\,E_c(x_n=0)\,|\,(C/\omega_n)^3\ . \tag{5}$$

Figure 1 shows two examples of our calculated correction function $E_c(x_n)$ compared with the corresponding short-time Gaussian form $\Delta l_G(x_n)$ from

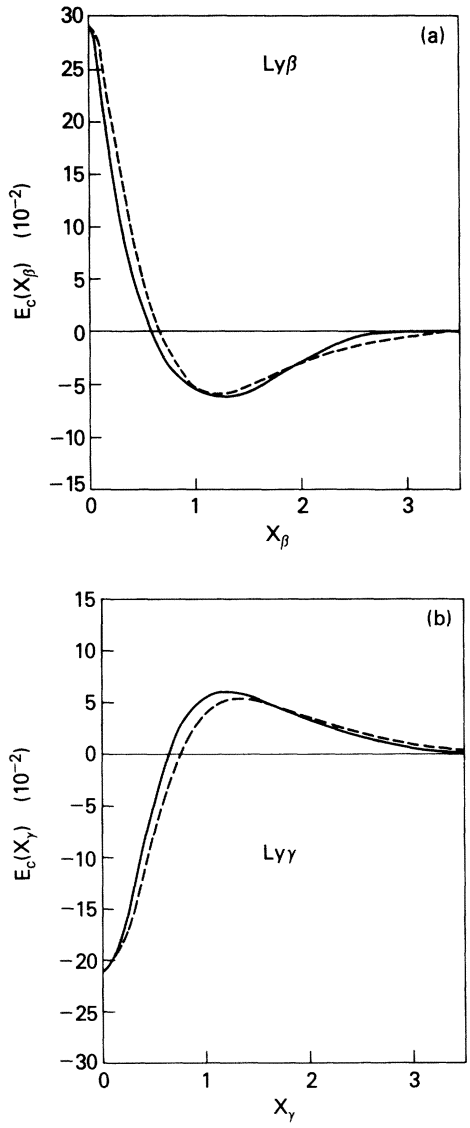

FIG. 1. Profile correction functions $E_c(x_n)$, solid curves, compared with the short-time Gaussian form of Eq. (4), dashed curves, as functions of x_n for (a) Lyman-β and (b) Lyman-γ of hydrogen at $N_e=10^{17}$ cm^{-3} and $T=12\,700$ K. C is taken to be the collision width of (a) the nearest shifted component and (b) the unshifted component. b is chosen so that the forms are equal at $x_n=0$.

Eq. (4) using b from Eq. (5) in the definition of ω_G, but reserving C as a fitting parameter. In Fig. 1(a), C is taken to be the electron collision width of the nearest shifted component of Lyman-β; in Fig. 1(b), C is equal to the electron collision width of the unshifted component of Lyman-γ. The fit is readily seen to be quite good, indicating that the second-order Gaussian approximation is very similar to our second-order analytic result provided C is selected with care. We now "sum" or, rather, extrapolate to all orders to obtain the full Gaussian [Eq. (3)] and use this for the low-frequency field Stark broadening function.

All that remains is to average this Stark profile, a Gaussian in frequency, over radiator velocities allowing for the Doppler shift and to convolve this averaged low-frequency Stark profile with the electron collision, quasistatic ion broadened profile. For small ratios of the masses of radiating to perturbing ions, we have

$$\omega_G=2\omega_n(b\epsilon^{(1)})^{1/2}=\frac{2}{r_0}\left[\frac{bk_BT}{M_r}\right]^{1/2}\frac{v}{v_r}\equiv\omega_G'\frac{v}{v_r}\ ,\quad v_r^2=\frac{k_BT}{M_r}\ . \tag{6}$$

The velocity averaged Stark profile in this case is identical with Eq. (33) of Ref. 7, except that ω_G' is defined according to Eq. (6). For $M_r/M_i\gg1$, the corresponding profile is a Gaussian of $1/e$ width

$$\omega_T=(\omega_G''^2+\omega_D^2)^{1/2} \tag{7}$$

with low-frequency Stark width

$$\omega_G''=\sqrt{3}\omega_G'=\frac{2}{r_0}\left[\frac{3bk_BT}{M_i}\right]^{1/2} \tag{8}$$

and Doppler width

$$\omega_D\equiv\left[\frac{2k_BT}{M_r}\right]^{1/2}\frac{\omega_0}{c}\ . \tag{9}$$

III. RESULTS AND DISCUSSION

The function $E_c(x_n)$ depends in a very complicated way on the electron collision width, so that $E_c(x_n)$, and thus C and b, are different for each choice of density, temperature, and radiator charge for a given line. In practice, the selection of C as the collision width of the unshifted component in Lyman-α and -γ and the width of the nearest shifted component in Lyman-β is adequate throughout the range of cases treated here. For Lyman-δ, C must be fit for each set of conditions. We have calculated the parameter b from Eq. (5) at several densities and temperatures for atomic hydrogen and hydrogenic helium, carbon, and argon radiators. The results are presented in Table I and we note that our calculations of b values, e.g., for Ne X indicate that interpolation from C VI to Ar XVIII is possible for a given line and for densities and temperatures scaled according to Ref. 13.

TABLE I. The parameter b defined by Eq. (5) for the first four lines of the Lyman series of atomic hydrogen and hydrogenic helium, carbon, and argon. In the case of hydrogen and helium lines, the perturbing ions are Ar^+, in the case of carbon and argon lines equal concentrations of D^+ and T^+. Column headings are the same for H and He II and for C VI and Ar XVIII.

$\log_{10}(N_e)$	$T(10^4\,K)$	α	β	γ	δ	$\log_{10}(N_e)$	$T(10^6\,K)$	α	β	γ	δ
		H						C VI			
16	0.5		0.921	1.636	3.93	19	0.5		0.136	1.188	1.18
	1		0.694	1.545	3.66		1		0.079	1.121	0.85
	2		0.508	1.463	3.31		2		0.045	1.076	0.47
17	0.5	0.614	1.348	1.748	3.79	20	0.5	0.546	0.339	1.324	1.96
	1	0.583	1.191	1.668	4.08		1	0.532	0.207	1.230	1.38
	2	0.560	0.998	1.595	4.02		2	0.522	0.125	1.156	0.94
	3		0.889								
18	0.5	0.651	1.441	1.813	3.74	21	0.5	0.563	0.688	1.453	2.13
	1	0.607	1.582	1.760	3.67		1	0.546	0.454	1.346	1.72
	2	0.576	1.537	1.684	4.08		2	0.533	0.312	1.255	1.31
19	0.5	0.712				22	0.5	0.579			
	1	0.665					1	0.562			
	2	0.595					2	0.546			
		He II						Ar XVIII			
17	2		0.841	1.582	3.92	22	4.5		0.109	1.162	0.79
	4		0.534	1.469	3.32		9		0.064	1.105	0.52
	8		0.329	1.359	2.34		18		0.038	1.065	0.33
18	2	0.600	1.596	1.678	4.50	23	4.5	0.549	0.251	1.259	0.96
	4	0.566	1.113	1.608	3.84		9	0.535	0.157	1.181	0.72
	8	0.550	0.745	1.512	3.33		18	0.524	0.095	1.124	0.52
19	2	0.621	2.343	1.740	4.50	24	4.5	0.569	0.435	1.315	0.72
	4	0.590	1.820	1.689	4.02		9	0.550	0.295	1.239	0.49
	8	0.560	1.339	1.616	3.54		18	0.535	0.195	1.175	0.40
20	2	0.635				25	4.5	0.594			
	4	0.598					9	0.570			
	8	0.604					18	0.551			

The parameter b is seen to be a slowly varying function of density and temperature, indicating relative insensitivity of the Gaussian extrapolation to the collision widths. This is desirable since the second-order Stark shape [see Eq. (4)] is quite sensitive to small changes in C. The present treatment of the α line does not require the simplifying assumptions made earlier.[7] In that paper the parameter equivalent to our b is a constant and equal to $(\frac{5}{4}\sqrt{3})^2=0.521$. This value is close enough to our tabulated values so that our profiles are essentially identical to those of Ref. 7. The values of b were arbitrarily varied to observe changes in the final convolved profiles. A 25% change in b leads to an intensity change at line center in Lyman-β of about 10%, with a 5% change at the peaks. The same percentage modification of b causes line center intensities in Lyman-γ and Lyman-δ to adjust by about 2% or less.

Before presenting results of profile calculations, we observe that Eqs. (6) and (8) correspond to Gaussian widths in the α scale[1,13] of

$$\alpha_G \approx \frac{r_0\lambda^2}{\pi c e}\left[\frac{3bk_BT}{M'}\right]^{1/2} = \frac{16\pi r_0 a_0^2 (3bk_BT/M')^{1/2}}{Z^4\alpha^2 c e (1-1/n^2)^2}\,, \tag{10}$$

where M' is the smaller of radiator or perturber

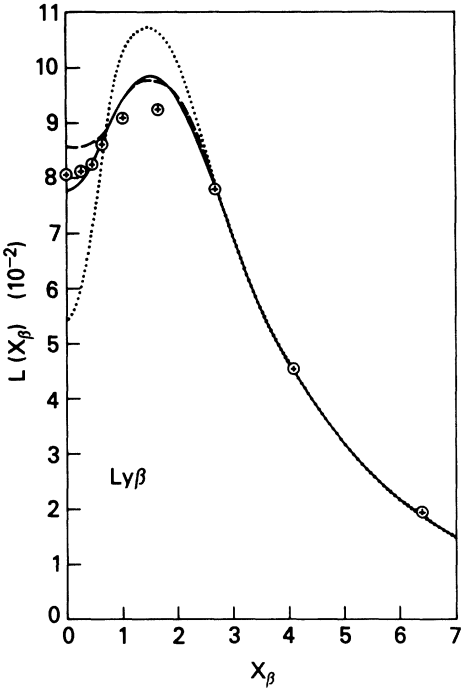

FIG. 2. Comparison of the second-order corrected line shape (dashed curve) with the "summed" Gaussian model considered here (solid) for Lyman-β of hydrogen at $N_e = 10^{17}$ cm^{-3} and $T = 12\,700$ K. Points are the measurements of Grützmacher and Wende (Ref. 5). Solid curve is the result of convolution of the correction function with the uncorrected profile of Ref. 3 (dots).

mass. These widths are of the same order of magnitude as an earlier estimate[13,14] α_C for low-frequency Stark broadening, but scale differently with plasma conditions, and are larger than α_C for relatively small perturber masses. All of these differences are as expected, because the earlier estimate allowed explicitly only for collective fields through a weak coupling approximation.

In Fig. 2 we compare the profile of Lyman-β of hydrogen in argon obtained from the Gaussian extrapolation with that obtained from the second-order calculation[9] at the conditions of the experiment.[5,6] Agreement is seen to be very good between experiment and both calculations, the second-order result predicting a slightly higher central intensity. Figure 3 shows our results for Lyman-δ of hydrogen in argon at conditions of the Lyman-β measurement. The profile correction is seen to be very small. The second-order correction, however, is unphysically large. Measurements are available[10] for Lyman-γ of hydrogen in argon at a density and temperature similar to the above, where again the second-order correction is inappropriate. Figure 4

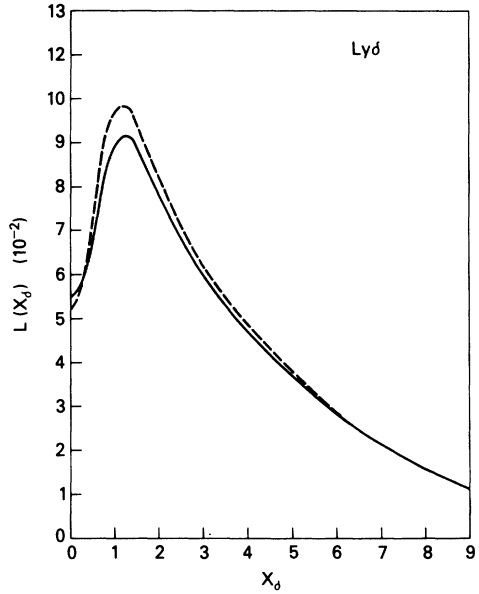

FIG. 3. Corrected profile (solid curve) of Lyman-δ of hydrogen at $N_e = 10^{17}$ cm^{-3} and $T = 12\,700$ K. Dashed curve is the uncorrected profile of Ref. 2.

compares the prediction by the Gaussian model and those measurements.

We conclude by presenting profiles of Lyman-α, -β, -γ, and -δ of Ar XVIII in a DT plasma for laser

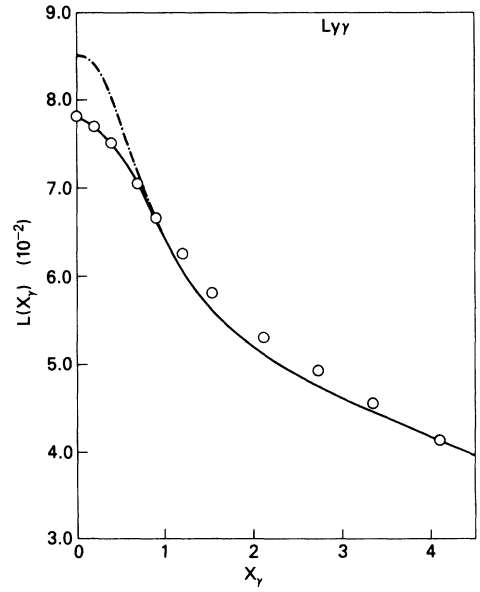

FIG. 4. Comparison of the model profile (solid curve) with measurements (Ref. 10) of Lyman-γ of hydrogen in argon at $N_e = 10^{17}$ cm^{-3} and $T = 12\,700$ K. Dashed curve is the uncorrected profile (Ref. 2) to which the correction function is applied.

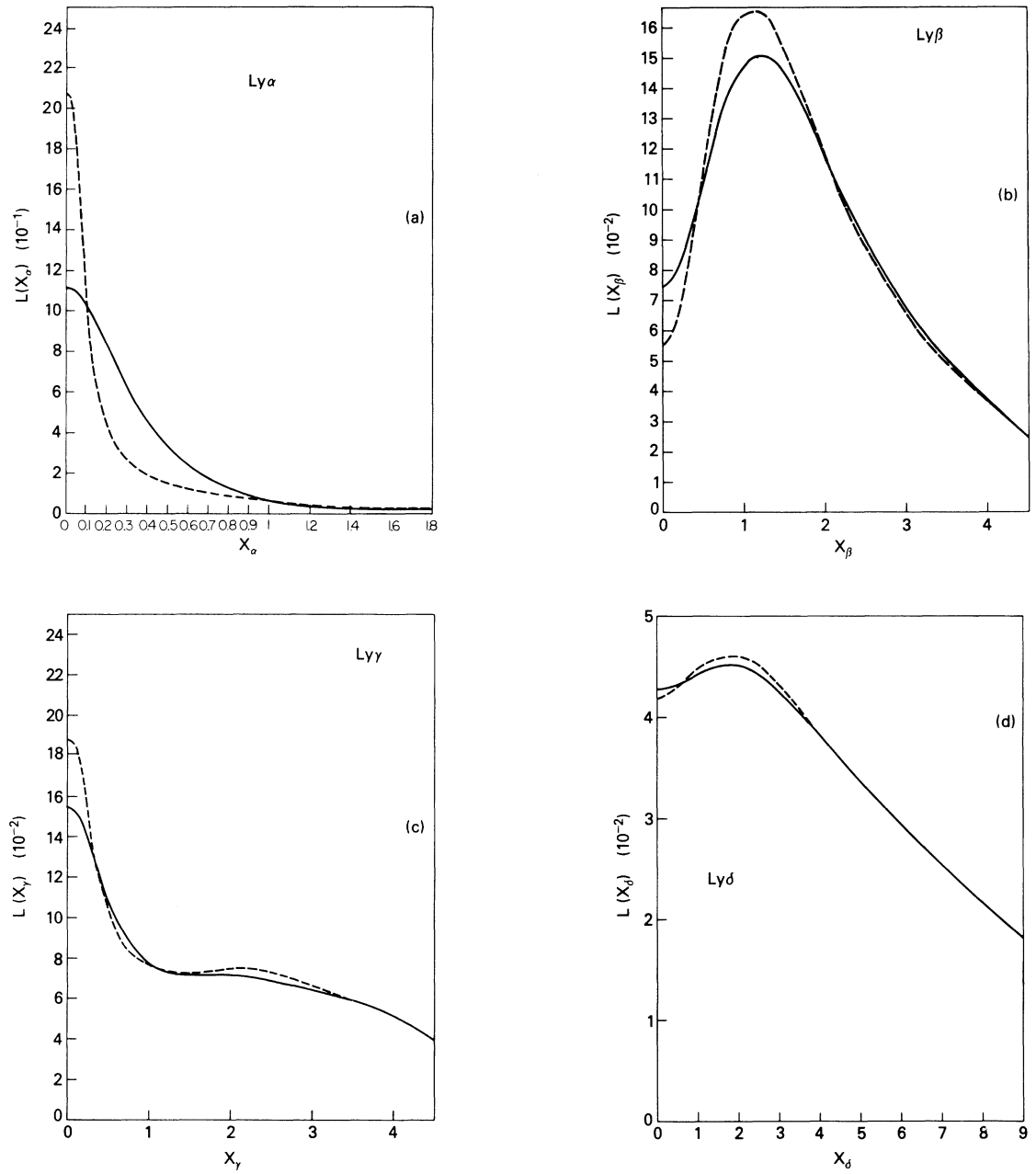

FIG. 5. Lyman-α (a), Lyman-β (b), Lyman-γ (c), and Lyman-δ (d) for Ar XVIII in a DT plasma at $N_e = 5\times10^{23}$ cm^{-3} and $T = 4.6\times10^6$ K. Dashed curves are modified impact broadened profiles (Ref. 14). Solid curves are the corrected profiles.

fusion experiments. We have calculated the line shapes at an electron density of 5×10^{23} cm^{-3} and temperature of 4.6×10^6 K. The modified impact profile[5] with which the Gaussian-Stark function is convolved is shown as the dashed curves in Fig. 5. The solid curves show the modification of the line shapes when ion motion and low-frequency electron field corrections are made via the model presented here. Fine-structure splitting was neglected in our calculations. It would have considerable effect on Lyman-α of Ar XVIII, for which the fine-structure splitting in units of ω_n is

$$\Delta x_F = \frac{\alpha^2 Z^5}{192}\left[\frac{4\pi}{3}Na_0^3\right]^{-2/3},$$

or $\Delta x_F \approx 1.15$ for the condition of Fig. 5. For higher members of the spectral series, errors from neglecting fine structure should be almost negligible, because Δx_F for them is smaller by a factor $\sim(2/n)^4$.

ACKNOWLEDGMENTS

We would like to acknowledge the assistance of Paul C. Kepple in discussing some aspects of this work. This work was supported by the U. S. Office of Naval Research and by the National Science Foundation

APPENDIX

In this appendix we present some details of the calculation of the line-shape correction for Lyman-α, -γ, and -δ including the definitions of the parabolic wave functions used to form the atomic matrix elements. Also presented is an outline of the solution of the coupled Schrödinger equations for the matrix elements.

In terms of the Fourier transformed time development operator, the second-order expression for the line-shape correction of a Lyman resonance line (of upper level n) is given by

$$\Delta L(\omega)=\frac{1}{3\pi}\mathrm{Re}\left\langle \sum_{s=0}^{n-1}\sum_{s'=0}^{n-1} z_{ss'}\tilde{U}^{(2)}_{ss'}\Big|_{m=0} + 2\sum_{s=0}^{n-2}\sum_{s'=0}^{n-2}\Gamma^{+}_{ss'}\tilde{U}^{(2)}_{ss'}\Big|_{m=1}\right\rangle , \tag{A1}$$

where

$$z_{ss'}\equiv\langle ns0\,|\,z\,|\,100\rangle\langle ns'0\,|\,z\,|\,100\rangle/N_z$$

and

$$\Gamma^{+}_{ss'}\equiv\langle ns1\,|\,(x+iy)\,|\,100\rangle\langle ns'1\,|\,(x+iy)\,|\,100\rangle/N_{\Gamma+} \tag{A1'}$$

are matrix elements (using parabolic wave functions, $|\,nsm\,\rangle$) of the dipole operator and $\tilde{U}^{(2)}_{ss'}$ is the corresponding matrix element of the second-order time development operator, e.g.,

$$\tilde{U}^{(2)}_{ss'}\,|_{m=0}\equiv\langle ns0\,|\,\tilde{U}^{(2)}\,|\,ns'0\rangle . \tag{A1''}$$

N_z and $N_{\Gamma+}$ in (A1') are normalizations. $\tilde{U}^{(2)}_{ss'}$ is the solution to second order of

$$-i(\Delta\omega-\omega_k)\tilde{U}_{k1}+\sum_l C_{kl}\tilde{U}_{lj} =\delta_{kj}-\dot{\omega}_{kk}\tilde{U}'_{kj}-\sum_{\substack{m\\ m\neq k}}\dot{\omega}_{km}\tilde{U}'_{mj} , \tag{A2}$$

where C_{kl} is the electron collision matrix, ω_k is the Stark shift in the initial field, and the $\dot{\omega}$ are proportional to the field derivatives.

$\Delta L(\omega)$ is thus given by a linear combination of $\langle\tilde{U}^{(2)}_{kl}\rangle$'s, the number of which is governed by the values of the matrix elements defined in Eq. (A1''). However, owing to a symmetry with respect to replacement of the initial field $\vec{F}$ by $-\vec{F}$ in Eq. (A2), only about one half that number of elements are needed. For example, applying Eq. (A1) to Lyman-α using the definitions given below gives the result

$$L_\alpha(\omega)=\frac{1}{3\pi}\mathrm{Re}\langle\tfrac{1}{2}(\tilde{U}_{11}+\tilde{U}_{22}-\tilde{U}_{21}-\tilde{U}_{12})+2\tilde{U}_{33}\rangle . \tag{A3}$$

After compensations due to the above-mentioned symmetry, the line shape is given by Eq. (A5). Since all of the U functions we will present below are Fourier transformed in time, in order to conserve space we will henceforth omit the tildes identifying the transform.

1. Lyman α

The parabolic wave functions ($|\,nsm\,\rangle$) for $n=2$ are defined in terms of spherical wave functions ($|\,nlm\,\rangle$) by

$$\left.\begin{aligned}|\,1\rangle\\ |\,2\rangle\end{aligned}\right\}=\frac{1}{\sqrt{2}}|\,200\rangle\pm\frac{1}{\sqrt{2}}|\,210\rangle ,$$
$$\left.\begin{aligned}|\,3\rangle\\ |\,4\rangle\end{aligned}\right\}=|\,21,\pm1\rangle . \tag{A4}$$

(These definitions differ slightly from Ref. 7.) The entire line shape according to Eq. (A1) is then

$$L_\alpha(\omega)=\frac{1}{3\pi}\mathrm{Re}\langle U_{11}-U_{21}+2U_{33}\rangle . \tag{A5}$$

The Stark shifts for the shifted components are given by

$$\omega_1=-\frac{3\hbar}{Zme}F \text{ and } \omega_2=-\omega_1 . \tag{A6}$$

The electron impact width of each component involves the matrix element of $\vec{R}\cdot\vec{R}$, where $\vec{R}$ is the position vector of the radiating electron. This quantity is diagonal in the spherical representation.[1] Thus using (A4), $\langle l\,|\,\vec{R}\cdot\vec{R}\,|\,k\rangle$ is seen to be

l \ k	1	2
1	2	2
2	1	1

where the matrix elements are in units of

$$C=9a_0^2. \tag{A7}$$

The matrix elements of $\dot{\omega}$ in Eq. (A2) are given by

$$\dot{\omega}_{kl}=\frac{-\hbar}{Zmea_0}\langle k\,|\,x\dot{F}_x+y\dot{F}_y+z\dot{F}_z\,|\,l\rangle\ . \tag{A8}$$

Since the initial field is assumed to lie in the z direction,

$$\dot{\omega}_{11}=-3\frac{\hbar}{Zme}\dot{F}_z=-3\frac{\hbar}{Zme}\dot{F}_{||}=-\dot{\omega}_{22}\ . \tag{A9}$$

The off-diagonal elements of $\dot{\omega}$ can be written[11]

$$\sum_k{}'\dot{\omega}_{1k}\dot{\omega}_{kl}=\left[\frac{\hbar}{mea_0Z}\right]^2\sum_k{}'\langle 1\,|\,(x\dot{F}_x+y\dot{F}_y)\,|\,k\rangle\langle k\,|\,(x\dot{F}_x+y\dot{F}_y)\,|\,l\rangle$$

$$\rightarrow\frac{1}{4}\left[\frac{\hbar}{mea_0Z}\right]^2\dot{F}_\perp^2\sum_k[\langle 1\,|\,\Gamma^+\,|\,k\rangle\langle k\,|\,\Gamma^-\,|\,l\rangle+\langle 1\,|\,\Gamma^-\,|\,k\rangle\langle k\,|\,\Gamma^+\,|\,l\rangle]\ , \tag{A10}$$

where $\Gamma^\pm=x\pm iy$. The two expressions in (A10) are equal when averages over cross terms (i.e., F_xF_y) are zero and $\dot{F}_x^2=\dot{F}_y^2=\frac{1}{2}F_\perp^2$. The matrix elements of Γ^+ and Γ^- for the states defined in (A4) are

	Γ^-					Γ^+				
l \ k	1	2	3	4	l \ k	1	2	3	4
1	0	0	1	0	1	0	0	0	1
2	0	0	1	0	2	0	0	0	1
3	0	0	0	0	3	1	1	0	0
4	1	1	0	0	4	0	0	0	0

where the elements are in units of $-3a_0$. It is readily seen that

$$\frac{\dot{\omega}_{13}\dot{\omega}_{31}}{\dot{\omega}_{11}^2}=\frac{1}{4}\left[\frac{\dot{F}_\perp}{F}\right]^2. \tag{A11}$$

We now must solve Eq. (A2) to second order in the interaction $\dot{\omega}$. For the elements U_{11} and U_{21} we proceed as follows. Define the matrix of the left-hand side (LHS) of (A2) using (A6), (A7), and the table of $\vec{R}\cdot\vec{R}$ matrix elements as

$$\underline{A}=\begin{bmatrix}2C-i(\Delta\omega-\omega_1) & C\\ C & 2C-i(\Delta\omega+\omega_1)\end{bmatrix}. \tag{A12}$$

The zeroth-order solution to U_{kl} is obtained by setting the derivatives in (A2) equal to zero. Thus

$$\begin{bmatrix}U_{11}^{(0)}\\ U_{21}^{(0)}\end{bmatrix}=\underline{A}^{-1}\begin{bmatrix}1\\0\end{bmatrix}.$$

Since the zeroth-order solution only connects states of equal quantum number m, the derivatives of this solution placed in the first $\dot{\omega}$ term on the right-hand side (RHS) of (A2) with the second $\dot{\omega}$ term on the RHS set equal to zero produce the first-order correction,

$$\begin{bmatrix}U_{11}^{(1)}\\ U_{21}^{(1)}\end{bmatrix}=\underline{A}^{-1}\begin{bmatrix}-\dot{\omega}_{11}U_{11}^{(0)'}\\ \omega_{11}U_{21}^{(0)'}\end{bmatrix}. \tag{A13}$$

The last term in (A2) couples states of different m so that it does not contribute to this order. To obtain the first-order contributions of these elements, a subequation of (A2) must be solved,

$$-i(\Delta\omega_m-\omega_m)U_{mj}^{(1)}+\sum_r C_{mr}U_{rj}^{(1)}=-\sum_r{}'\dot{\omega}_{mr}U_{rj}^{(0)'}\ . \tag{A14}$$

For Lyman-α (A14) reduces to

$$(C-i\Delta\omega)U_{31}^{(1)}=-\dot{\omega}_{31}(U_{11}^{(0)'}+U_{21}^{(0)'})\ . \tag{A15}$$

Substituting the derivatives of the solutions to (A13) and (A15) into the RHS of (A2) gives the needed second-order correction

$$\begin{bmatrix}U_{11}^{(2)}\\ U_{21}^{(2)}\end{bmatrix}=\underline{A}^{-1}\begin{bmatrix}-\dot{\omega}_{11}U_{11}^{(1)'}-2\dot{\omega}_{13}U_{31}^{(1)'}\\ \dot{\omega}_{11}U_{21}^{(1)'}-2\dot{\omega}_{13}U_{31}^{(1)'}\end{bmatrix}. \tag{A16}$$

The third needed matrix-element correction $U_{33}^{(2)}$ is

$$U_{33}^{(2)}=\frac{-\dot{\omega}_{31}}{(C-i\Delta\omega)}(U_{13}^{(1)'}+U_{23}^{(1)'})\ , \tag{A17}$$

where

$$\begin{bmatrix} U_{13}^{(1)} \\ U_{23}^{(1)} \end{bmatrix} = -\underline{A}^{-1} \frac{2i\dot{\omega}_{13}}{(C-i\Delta\omega)^2} \underline{I} .$$

Rewriting Eq. (A5) as

$$\begin{aligned} L_\alpha(\omega) &= \frac{1}{3\pi} \mathrm{Re}\langle U_{11}^{(0)} + U_{11}^{(2)} - U_{21}^{(0)} \\ &\quad - U_{21}^{(2)} + 2U_{33}^{(0)} + 2U_{33}^{(2)} \rangle \\ &= L_\alpha^{(0)}(\omega) + \Delta L_\alpha(\omega) , \end{aligned} \tag{A18}$$

where we note that the first-order U's vanish in the field average, and the second-order correction to the line shape can be obtained from Eqs. (A18), (A16), and (A17).

2. Lyman γ

Application of Eq. (A1) to the Lyman-γ resonance line leads to the following form of the correction to the line shape:

$$\begin{aligned} \Delta L_\gamma(\omega) = \frac{1}{3\pi} \mathrm{Re}\langle \tfrac{1}{10}[9(U_{11}^{(2)} - U_{41}^{(2)}) + U_{22}^{(2)} - U_{32}^{(2)} + 3(U_{21}^{(2)} + U_{12}^{(2)} - U_{42}^{(2)} - U_{31}^{(2)})] \\ + 4[0.301(U_{55}^{(2)} + U_{75}^{(2)}) + 0.199U_{66}^{(2)} + 0.346(U_{65}^{(2)} + U_{76}^{(2)})]\rangle . \end{aligned} \tag{A19}$$

The parabolic wave functions used in (A19) are defined in terms of spherical wave functions as

$$\left.\begin{matrix} |1\rangle \\ |4\rangle \end{matrix}\right\} = \tfrac{1}{2}|400\rangle \pm \frac{3}{\sqrt{20}}|410\rangle + \tfrac{1}{2}|420\rangle \pm \frac{1}{\sqrt{20}}|430\rangle ,$$

$$\left.\begin{matrix} |2\rangle \\ |3\rangle \end{matrix}\right\} = \tfrac{1}{2}|400\rangle \pm \frac{1}{\sqrt{20}}|410\rangle - \tfrac{1}{2}|420\rangle \mp \frac{3}{\sqrt{20}}|430\rangle ,$$

$$\left.\begin{matrix} |5\rangle, |8\rangle \\ |7\rangle, |10\rangle \end{matrix}\right\} = (\tfrac{3}{10})^{1/2}|41,\pm1\rangle \pm \frac{1}{\sqrt{2}}|42,\pm1\rangle + \frac{1}{\sqrt{5}}|43,\pm1\rangle ,$$

$$|6\rangle, |9\rangle = (\tfrac{2}{5})^{1/2}|41,\pm1\rangle - (\tfrac{3}{5})^{1/2}|43,\pm1\rangle ,$$

$$\left.\begin{matrix} |11\rangle, |13\rangle \\ |12\rangle, |14\rangle \end{matrix}\right\} = \frac{1}{\sqrt{2}}|42,\pm2\rangle \pm \frac{1}{\sqrt{2}}|43,\pm2\rangle ,$$

$$|15\rangle, |16\rangle = |43\pm3\rangle . \tag{A20}$$

The Stark shifts of the various components are given by

$$\begin{aligned} &\omega_1 = -\omega_4 = 3\omega_2 , \\ &\omega_3 = \omega_{12} = -\omega_{11} = -\omega_2 , \\ &\omega_5 = -\omega_7 = 2\omega_2 , \end{aligned} \tag{A21a}$$

where

$$\omega_2 = -6\frac{\hbar}{Zme}F \tag{A21b}$$

is the smallest nonzero Stark shift.

The diagonal elements of $\dot{\omega}$ will have the same prefactors as in Eq. (A21a) with

$$\dot{\omega}_{22} = -6\frac{\hbar}{Zme}\dot{F}_{||} . \tag{A22}$$

A table of off-diagonal elements [involving Γ^+ and Γ^-—see Eq. (A10) and comments thereafter] can be constructed. The elements are found to have two distinct evaluations which we label

$$\dot{\omega}_{15} = -6\sqrt{3}\frac{\hbar}{Zme}\dot{F}_\perp$$

and

$$\dot{\omega}_{36} = -12\frac{\hbar}{Zme}\dot{F}_\perp . \tag{A23}$$

Taking $\dot{\omega}_{15}$ as the basis we find that according to Eq. (A10)

$$\frac{\dot{\omega}_{15}\dot{\omega}_{51}}{\dot{\omega}_{22}^2} = \tfrac{3}{4}\left[\frac{\dot{F}_\perp}{F}\right]^2 . \tag{A24}$$

Atomic matrix elements of $\vec{R}\cdot\vec{R}$ are all proportional to a width C, which we take to be one-third the value of C_{12}, i.e.,

$$C = 36a_0^2 . \tag{A25}$$

These matrix elements couple to as many as two off-diagonal states, thus the LHS of Eq. (A2) is tridiagonal. In addition, the LHS forms a symmetric matrix. We need all of the U elements in Eq. (A19) as solutions of (A2) and U elements that these couple to through the last term in (A2). We define the following "left-hand sides" of (A2) as

$$\underline{A}=\begin{bmatrix} 12C-i(\Delta\omega-3\omega_2) & 3C & 0 & 0 \\ 3C & 8C-i(\Delta\omega-\omega_2) & 4C & 0 \\ 0 & 4C & 8C-i(\Delta\omega+\omega_2) & 3C \\ 0 & 0 & 3C & 12C-i(\Delta\omega+3\omega_2) \end{bmatrix},$$

$$\underline{B}=\begin{bmatrix} 9C-i(\Delta\omega-2\omega_2) & 2\sqrt{3}C & 0 \\ 2\sqrt{3}C & 7C-i\Delta\omega & 2\sqrt{3}C \\ 0 & 2\sqrt{3}C & 9C-i(\Delta\omega+2\omega_2) \end{bmatrix}, \tag{A26}$$

and

$$\underline{C}=\begin{bmatrix} 6C-i(\Delta\omega-\omega_2) & 3C \\ 3C & 6C-i(\Delta\omega+\omega_2) \end{bmatrix}.$$

Zero order. The zeroth-order U's required by (A19) are found by inverting

$$\underline{A}\begin{bmatrix} U_{11}^{(0)} \\ U_{21}^{(0)} \\ U_{31}^{(0)} \\ U_{41}^{(0)} \end{bmatrix}=\begin{bmatrix} 1 \\ 0 \\ 0 \\ 0 \end{bmatrix};\quad \underline{B}\begin{bmatrix} U_{55}^{(0)} \\ U_{65}^{(0)} \\ U_{75}^{(0)} \end{bmatrix}\begin{bmatrix} 1 \\ 0 \\ 0 \end{bmatrix}. \tag{A27a}$$

The solutions of $U_{rs}^{(0)}$ with column indices (s) equal to 2 and 6, respectively, are found from Eq. (A27a) with the RHS's of (A27a) equal to

$$\begin{bmatrix} 0 \\ 1 \\ 0 \\ 0 \end{bmatrix} \text{ and } \begin{bmatrix} 0 \\ 1 \\ 0 \end{bmatrix}, \tag{A27b}$$

respectively.

First order. In first order we have

$$\begin{bmatrix} U_{1i}^{(1)} \\ U_{2i}^{(1)} \\ U_{3i}^{(1)} \\ U_{4i}^{(1)} \end{bmatrix}=\underline{A}^{-1}\begin{bmatrix} -3\dot{\omega}_{22}U_{1i}^{(0)'} \\ -\dot{\omega}_{22}U_{2i}^{(0)'} \\ \dot{\omega}_{22}U_{3i}^{(0)'} \\ 3\dot{\omega}_{22}U_{4i}^{(0)'} \end{bmatrix},\quad i=1,2 \tag{A28a}$$

and

$$\begin{bmatrix} U_{5j}^{(1)} \\ U_{6j}^{(1)} \\ U_{7j}^{(1)} \end{bmatrix}=\underline{B}^{-1}\begin{bmatrix} -\dot{\omega}_{22}U_{5j}^{(0)'} \\ 0 \\ 2\dot{\omega}_{22}U_{7j}^{(0)'} \end{bmatrix},\quad j=5,6. \tag{A28b}$$

We will also require first-order contributions from terms that couple through different magnetic quantum numbers. We will need

$$\begin{bmatrix} U_{11,j}^{(1)} \\ U_{12,j}^{(1)} \end{bmatrix}=-\underline{C}^{-1}\begin{bmatrix} \dot{\omega}_{36}U_{5j}^{(0)'}+\dot{\omega}_{15}U_{6j}^{(0)'} \\ \dot{\omega}_{15}U_{6j}^{(0)'}+\omega_{36}U_{7j}^{(0)'} \end{bmatrix},\quad j=5,6 \tag{A28c}$$

$$\begin{bmatrix} U_{1j}^{(1)} \\ U_{2j}^{(1)} \\ U_{3j}^{(1)} \\ U_{4j}^{(1)} \end{bmatrix}=-\underline{A}^{-1}\begin{bmatrix} \dot{\omega}_{15}U_{5j}^{(0)'} \\ \dot{\omega}_{15}U_{5j}^{(0)'}+\dot{\omega}_{36}U_{7j}^{(0)'} \\ \dot{\omega}_{36}U_{6j}^{(0)'}+\dot{\omega}_{15}U_{7j}^{(0)'} \\ \dot{\omega}_{15}U_{7j}^{(0)'} \end{bmatrix},\quad j=5,6 \tag{A28d}$$

and

$$\begin{bmatrix} U_{5i}^{(1)} \\ U_{4i}^{(1)} \\ U_{7i}^{(1)} \end{bmatrix}=-\underline{B}^{-1}\begin{bmatrix} \dot{\omega}_{51}(U_{1i}^{(0)'}+U_{2i}^{(0)'}) \\ \dot{\omega}_{63}(U_{2i}^{(0)'}+U_{3i}^{(0)'}) \\ \dot{\omega}_{51}(U_{3i}^{(0)'}+U_{4i}^{(0)'}) \end{bmatrix},\quad i=1,2. \tag{A28e}$$

Second order. The required second-order U elements are seen to be

$$\begin{bmatrix} U_{1i}^{(2)} \\ U_{2i}^{(2)} \\ U_{3i}^{(2)} \\ U_{4i}^{(2)} \end{bmatrix}=\underline{A}^{-1}\begin{bmatrix} -3\dot{\omega}_{22}U_{1i}^{(1)'}-2\dot{\omega}_{15}U_{5i}^{(1)'} \\ -\dot{\omega}_{22}U^{(1)'}-2\dot{\omega}_{15}U_{5i}^{(1)'}-2\dot{\omega}_{36}U_{6i}^{(1)'} \\ \dot{\omega}_{22}U_{3i}^{(1)'}-2\dot{\omega}_{36}U_{6i}^{(1)'}-2\dot{\omega}_{15}U_{7i}^{(1)'} \\ 3\dot{\omega}_{22}U_{4i}^{(1)}-2\dot{\omega}_{15}U_{7i}^{(1)'} \end{bmatrix},\quad i=1,2 \tag{A29a}$$

and

$$\begin{bmatrix} U_{5j}^{(2)} \\ U_{4j}^{(2)} \\ U_{7j}^{(2)} \end{bmatrix} = \underline{B}^{-1} \begin{bmatrix} -2\dot{\omega}_{22}U_{5j}^{(1)'} - \dot{\omega}_{51}(U_{1j}^{(1)'} + U_{2j}^{(1)'}) - \dot{\omega}_{63}U_{11,j}^{(1)'} \\ -\dot{\omega}_{63}(U_{2j}^{(1)'} + U_{3j}^{(1)'}) - \dot{\omega}_{51}(U_{11,j}^{(1)'} + U_{12,j}^{(1)'}) \\ 2\dot{\omega}_{22}U_{7j}^{(1)'} - \dot{\omega}_{51}(U_{3j}^{(1)'} + U_{4j}^{(1)'}) - \dot{\omega}_{63}U_{12,j}^{(1)'} \end{bmatrix}, \quad j=5,6 . \tag{A29b}$$

The line-shape correction is found by inserting the derivatives with respect to $\Delta\omega$ of solutions of (A17) in (A28), taking derivatives in (A28) and inserting into the RHS of (A29), and replacing the $U_{rs}^{(2)}$'s in Eq. (A19) by the results of Eq. (A29).

3. Lyman δ

The line corrections for Lyman-δ found from Eq. (A1) is

$$\Delta L_\delta(\omega) = \frac{1}{3\pi}\mathrm{Re}\langle \tfrac{1}{5}[4(U_{11}^{(2)} - U_{51}^{(2)}) + U_{22}^{(2)} - U_{42}^{(2)} + 2(U_{12}^{(2)} + U_{21}^{(2)} - U_{41}^{(2)} - U_{52}^{(2)})] + 4[0.301(U_{66}^{(2)} + U_{96}^{(2)}) + 0.199(U_{77}^{(2)} + U_{87}^{(2)}) + 0.245(U_{67}^{(2)} + U_{76}^{(2)} + U_{86}^{(2)} + U_{97}^{(2)})]\rangle . \tag{A30}$$

The time development operator matrix elements in Eq. (A30) are found with respect to the parabolic wave functions defined in Eqs. (A31):

$$\left.\begin{matrix} |1\rangle \\ |5\rangle \end{matrix}\right\} = \frac{1}{\sqrt{5}}|500\rangle \pm (\tfrac{2}{5})^{1/2}|510\rangle + (\tfrac{2}{7})^{1/2}|520\rangle \pm \frac{1}{\sqrt{10}}|530\rangle + \frac{1}{\sqrt{70}}|540\rangle ,$$

$$\left.\begin{matrix} |2\rangle \\ |4\rangle \end{matrix}\right\} = \frac{1}{\sqrt{5}}|500\rangle \pm \frac{1}{\sqrt{10}}|510\rangle - (\tfrac{1}{14})^{1/2}|520\rangle \mp (\tfrac{2}{5})^{1/2}|530\rangle - (\tfrac{8}{35})^{1/2}|540\rangle ,$$

$$|3\rangle = \frac{1}{\sqrt{5}}|500\rangle - (\tfrac{2}{7})^{1/2}|520\rangle + (\tfrac{18}{35})^{1/2}|540\rangle ,$$

$$\left.\begin{matrix} |6\rangle, |10\rangle \\ |9\rangle, |13\rangle \end{matrix}\right\} = \frac{1}{\sqrt{5}}|51,\pm1\rangle \pm (\tfrac{3}{7})^{1/2}|52,\pm1\rangle + (\tfrac{3}{10})^{1/2}|53,\pm1\rangle \pm (\tfrac{1}{14})^{1/2}|54,\pm1\rangle ,$$

$$\left.\begin{matrix} |7\rangle, |11\rangle \\ |8\rangle, |13\rangle \end{matrix}\right\} = (\tfrac{3}{10})^{1/2}|51,\pm1\rangle \pm (\tfrac{1}{14})^{1/2}|52,\pm1\rangle - \frac{1}{\sqrt{5}}|53,\pm1\rangle \mp (\tfrac{3}{7})^{1/2}|54,\pm1\rangle , \tag{A31}$$

$$\left.\begin{matrix} |14\rangle, |17\rangle \\ |16\rangle, |19\rangle \end{matrix}\right\} = (\tfrac{2}{7})^{1/2}|52,\pm2\rangle \pm \frac{1}{\sqrt{2}}|53,\pm2\rangle + (\tfrac{3}{14})^{1/2}|54,\pm2\rangle ,$$

$$|15\rangle, |18\rangle = (\tfrac{3}{7})^{1/2}|52,\pm2\rangle - (\tfrac{4}{7})^{1/2}|54,\pm2\rangle ,$$

$$\left.\begin{matrix} |20\rangle, |22\rangle \\ |21\rangle, |23\rangle \end{matrix}\right\} = \frac{1}{\sqrt{2}}|53,\pm3\rangle \pm \frac{1}{\sqrt{2}}|54,\pm3\rangle ,$$

$$|24\rangle, |25\rangle = |54,\pm4\rangle .$$

With these definitions we find the Stark shifts of the various components as

$$\begin{aligned} &\omega_1 = -\omega_5 = 4\omega_7 , \\ &\omega_6 = -\omega_9 = 3\omega_7 , \\ &\omega_2 = -\omega_4 = \omega_{14} = -\omega_{16} = 2\omega_7 , \\ &\omega_{20} = -\omega_{21} = \omega_7 , \end{aligned} \tag{A32a}$$

where the least nonzero shift is given by

$$\omega_7 = -\frac{15}{2}\frac{\hbar}{Zme}F . \tag{A32b}$$

The diagonal elements of $\dot{\omega}$ possess the same prefactors as in Eq. (A32a) with

$$\dot{\omega}_{77} = -\frac{15}{2}\frac{\hbar}{Zme}\dot{F}_{||} . \tag{A33}$$

The various off-diagonal elements of $\dot{\omega}$ possess two distinct values. We represent these elements as

$$\dot{\omega}_{16} = -15\frac{\hbar}{Zme}\dot{F}_\perp$$

and

$$\dot{\omega}_{37} = -18.38\frac{\hbar}{Zme}\dot{F}_\perp . \tag{A34}$$

Using $\dot{\omega}_{16}$ as a basis we find that

$$\frac{\dot{\omega}_{16}\dot{\omega}_{61}}{\omega_{77}^2} = \left[\frac{\dot{F}_\perp}{F}\right]^2 . \tag{A35}$$

The matrix element of $\vec{R}\cdot\vec{R}$ between states $|1\rangle$ and $|2\rangle$ is

$$C_{12} = 225a_0^2 \equiv C . \tag{A36}$$

All other elements of $\vec{R}\cdot\vec{R}$ are proportional to C. The LHS matrices of Eq. (A1) that we require are given by Eqs. (A37):

$$\underline{A}=\begin{bmatrix} 5C-i(\Delta\omega-4\omega_7) & C & 0 & 0 & 0 \\ C & \frac{7}{2}C-(\Delta\omega-2\omega_7) & \frac{3}{2}C & 0 & 0 \\ 0 & \frac{3}{2}C & 3C-i\Delta\omega & \frac{3}{2}C & 0 \\ 0 & 0 & \frac{3}{2}C & \frac{7}{2}C-i(\Delta\omega+2\omega_7) & C \\ 0 & 0 & 0 & C & 5C-i(\Delta\omega+4\omega_7) \end{bmatrix},$$

$$\underline{B}=\begin{bmatrix} 4C-i(\Delta\omega-3\omega_7) & (\frac{3}{2})^{1/2}C & 0 & 0 \\ (\frac{3}{2})^{1/2}C & 3C-i(\Delta\omega-\omega_7) & \frac{3}{2}C & 0 \\ 0 & \frac{3}{2}C & 3C-i(\Delta\omega+\omega_7) & (\frac{3}{2})^{1/2}C \\ 0 & 0 & (\frac{2}{3})^{1/2}C & 4C-i(\Delta\omega+3\omega_7) \end{bmatrix}, \tag{A37}$$

$$\underline{C}=\begin{bmatrix} 3C-i(\Delta\omega-2\omega_7) & (\frac{3}{2})^{1/2}C & 0 \\ (\frac{3}{2})^{1/2}C & \frac{5}{2}C-i\Delta\omega & (\frac{3}{2})^{1/2}C \\ 0 & (\frac{3}{2})^{1/2}C & 3C-i(\Delta\omega+2\omega_7) \end{bmatrix}.$$

Zero order. In analogy with Eq. (A27a) for Lyman-γ, we solve

$$-i(\Delta\omega-\omega_k)U_{kl}^{(0)}+\sum_r C_{kr}U_{rl}^{(0)}=\delta_{kl} \tag{A38}$$

for all of the matrix elements listed in Eq. (A30). These are solutions of

$$\underline{A}\begin{bmatrix} U_{11}^{(0)} \\ U_{71}^{(0)} \\ U_{31}^{(0)} \\ U_{41}^{(0)} \\ U_{51}^{(0)} \end{bmatrix}=\begin{bmatrix} 1 \\ 0 \\ 0 \\ 0 \\ 0 \end{bmatrix};\quad \underline{B}\begin{bmatrix} U_{66}^{(0)} \\ U_{76}^{(0)} \\ U_{86}^{(0)} \\ U_{76}^{(0)} \end{bmatrix}=\begin{bmatrix} 1 \\ 0 \\ 0 \\ 0 \end{bmatrix}. \tag{A39a}$$

As before solutions of $U_{rs}^{(0)}$ with $s=2$ and 7 are, respectively, found from (A39a) with the RHS's of (A39a) replaced by

$$\begin{bmatrix} 0 \\ 1 \\ 0 \\ 0 \\ 0 \end{bmatrix}\quad\text{and}\quad\begin{bmatrix} 0 \\ 1 \\ 0 \\ 0 \end{bmatrix}, \tag{A39b}$$

respectively.

First order. In first order we have

$$\begin{bmatrix} U_{1i}^{(1)} \\ U_{2i}^{(1)} \\ U_{3i}^{(1)} \\ U_{4i}^{(1)} \\ U_{5i}^{(1)} \end{bmatrix}=\underline{A}^{-1}\begin{bmatrix} -4\dot{\omega}_{77}U_{1i}^{(0)'} \\ -2\dot{\omega}_{77}U_{2i}^{(0)'} \\ 0 \\ 2\dot{\omega}_{77}U_{5i}^{(0)'} \\ 4\dot{\omega}_{77}U_{5i}^{(0)'} \end{bmatrix},\quad i=1,2 \tag{A40a}$$

and

$$\begin{bmatrix} U_{6j}^{(1)} \\ U_{7j}^{(1)} \\ U_{8j}^{(1)} \\ U_{9j}^{(1)} \end{bmatrix}=\underline{B}^{-1}\begin{bmatrix} -3\dot{\omega}_{77}U_{6j}^{(0)'} \\ -\dot{\omega}_{77}U_{7j}^{(0)'} \\ \dot{\omega}_{77}U_{8j}^{(0)'} \\ 3\dot{\omega}_{77}U_{9j}^{(0)'} \end{bmatrix},\quad j=6,7. \tag{A40b}$$

For contributions in first order due to coupling distinct magnetic quantum numbers, we solve Eq. (A14) for all needed elements,

$$\begin{bmatrix} U_{14,j}^{(1)} \\ U_{15,j}^{(1)} \\ U_{16,j}^{(1)} \end{bmatrix}=-\underline{C}^{-1}\begin{bmatrix} \dot{\omega}_{73}U_{6j}^{(0)'}+\dot{\omega}_{61}U_{7j}^{(0)'} \\ \dot{\omega}_{73}(U_{7j}^{(0)'}+U_{8j}^{(0)'}) \\ \dot{\omega}_{61}U_{8j}^{(0)'}+\dot{\omega}_{73}U_{9j}^{(0)'} \end{bmatrix},\quad j=6,7 \tag{A40c}$$

$$\begin{bmatrix} U_{1j}^{(1)} \\ U_{2j}^{(1)} \\ U_{3j}^{(1)} \\ U_{4j}^{(1)} \\ U_{5j}^{(1)} \end{bmatrix} = -2\underline{A}^{-1} \begin{bmatrix} \dot{\omega}_{16} U_{6j}^{(0)'} \\ \dot{\omega}_{16} U_{6j}^{(0)'} + \dot{\omega}_{37} U_{7j}^{(0)'} \\ \dot{\omega}_{37}(U_{7j}^{(0)'} + U_{8j}^{(0)'}) \\ \dot{\omega}_{37} U_{8j}^{(0)'} + \dot{\omega}_{16} U_{9j}^{(0)'} \\ \dot{\omega}_{16} U_{9j}^{(0)'} \end{bmatrix}, \quad j=6,7 \tag{40d}$$

and

$$\begin{bmatrix} U_{6i}^{(1)} \\ U_{7i}^{(1)} \\ U_{8i}^{(1)} \\ U_{9i}^{(1)} \end{bmatrix} = -\underline{B} \begin{bmatrix} \dot{\omega}_{61}(U_{1i}^{(0)'} + U_{2i}^{(0)'}) \\ \dot{\omega}_{73}(U_{2i}^{(0)'} + U_{3i}^{(0)'}) \\ \dot{\omega}_{73}(U_{3i}^{(0)'} + U_{4i}^{(0)'}) \\ \dot{\omega}_{61}(U_{4i}^{(0)'} + U_{5i}^{(0)'}) \end{bmatrix}, \quad i=6,7 . \tag{40e}$$

Second order. The required second-order U elements are found as

$$\begin{bmatrix} U_{1i}^{(2)} \\ U_{2i}^{(2)} \\ U_{3i}^{(2)} \\ U_{4i}^{(2)} \\ U_{5i}^{(2)} \end{bmatrix} = \underline{A}^{-1} \begin{bmatrix} 4\dot{\omega}_{77} U_{1i}^{(1)'} - 2\dot{\omega}_{16} U_{6i}^{(1)'} \\ -2\dot{\omega}_{77} U_{2i}^{(1)'} - 2(\dot{\omega}_{16} U_{6i}^{(1)'} + \dot{\omega}_{37} U_{7i}^{(1)'} \\ -2\dot{\omega}_{37}(U_{7i}^{(1)'} + U_{8i}^{(1)'}) \\ 2\dot{\omega}_{77} U_{4i}^{(1)'} - 2(\dot{\omega}_{37} U_{8i}^{(1)'} + \dot{\omega}_{16} U_{4i}^{(1)'}) \\ 4\dot{\omega}_{77} U_{5i}^{(1)'} - 2\dot{\omega}_{16} U_{9i}^{(1)'} \end{bmatrix}, \quad i=1,2 \tag{A41a}$$

and

$$\begin{bmatrix} U_{6j}^{(2)} \\ U_{7j}^{(2)} \\ U_{8j}^{(2)} \\ U_{9j}^{(2)} \end{bmatrix} = \underline{B}^{-1} \begin{bmatrix} -3\dot{\omega}_{77} U_{6j}^{(1)'} - \dot{\omega}_{61}(U_{1j}^{(1)'} + U_{2j}^{(1)'}) + \dot{\omega}_{73} U_{14,j}^{(1)'} \\ -\dot{\omega}_{77} U_{7j}^{(1)'} - \dot{\omega}_{73}(U_{2j}^{(1)'} + U_{3j}^{(1)'} + U_{15,j}^{(1)'}) + \dot{\omega}_{61} U_{14,j}^{(1)'} \\ \dot{\omega}_{77} U_{8j}^{(1)'} - \dot{\omega}_{73}(U_{3j}^{(1)'} + U_{4j}^{(1)'} + U_{15,j}^{(1)'}) + \dot{\omega}_{61} U_{16,j}^{(1)'} \\ 3\dot{\omega}_{77} U_{9j}^{(1)'} - \dot{\omega}_{61}(U_{4j}^{(1)'} + U_{5j}^{(1)'}) + \dot{\omega}_{73} U_{16,j}^{(1)'} \end{bmatrix}, \quad j=6,7 . \tag{A41b}$$

The second-order line shape is then found by inserting (A41), (A40), and (A39) in Eq. (A30).

[1] H. R. Griem, *Spectral Line Broadening by Plasmas* (Academic, New York, 1974).

[2] P. Kepple and H. R. Griem, Phys. Rev. 173, 317 (1968).

[3] C. R. Vidal, J. Cooper, and E. W. Smith, Astrophys. J. Suppl. Ser. 25, 37 (1973).

[4] W. L. Wiese, D. E. Kelleher, and V. Helbig, Phys. Rev. A 11, 1858 (1975).

[5] K. Grützmacher and B. Wende, Phys. Rev. A 16, 243 (1977); A 18, 2140 (1978).

[6] R. Stamm and D. Voslamber, J. Quant. Spectrosc. Radiat. Transfer 22, 599 (1979).

[7] H. R. Griem, Phys. Rev. A 20, 606 (1979).

[8] S. Chandrasekhar and J. von Neumann, Astrophys. J. 95, 489 (1942); 97, 1 (1943).

[9] H. R. Griem and G. D. Tsakiris, Phys. Rev. A 25, 1199 (1982).

[10] M. Geisler, K. Grützmacher, and B. Wende in *Spectral Line Shapes*, edited by B. Wende (de Gruyter, Berlin, 1981), p. 103.

[11] H. R. Griem and G. D. Tsakiris, University of Maryland Plasma Group Report No. PL-80-021, 1980 (unpublished).

[12] R. L. Greene, J. Quant. Spectrosc. Radiat. Transfer 27, 185 (1982); 27, 639 (1982).

[13] H. R. Griem, M. Blaha, and P. C. Kepple, Phys. Rev. A 19, 2421 (1979).

[14] H. R. Griem, Phys. Rev. A 17, 214 (1978).

[15] P. C. Kepple and K. G. Whitney, Naval Research Laboratory Memorandum Report No. 4565, 1981 (unpublished).